Measurements of Craze Velocities in Polystyrene–Polybutadiene Blends

STEPHEN H. SPIEGELBERG,[1] ALI S. ARGON,[2] and ROBERT E. COHEN[1,*]

[1]Department of Chemical Engineering and [2]Department of Mechanical Engineering,
Massachusetts Institute of Technology, Cambridge, Massachusetts 02139

SYNOPSIS

Normally brittle polystyrene (PS) can be toughened effectively by the inclusion of a few weight percent of low molecular weight polybutadiene (PB). The PB, which can be made to phase separate into submicron sized, randomly dispersed pools, locally plasticizes the glassy phase in the vicinity of a growing craze; the resulting reduction in craze flow stress and increased craze velocity lead to significant enhancement of toughness when strain rates are below approximately 10^{-1} s^{-1}. Craze velocities were measured in PS containing 1 to 5 wt % of a low molecular weight PB (2300 g/mol). The results were compared to a version of the interface convolution mechanism for craze growth that has been modified to account for the localized plasticization effect of the low molecular weight diluent. Addition of 5 wt % PB led to craze velocities that are three orders of magnitude larger than observed for pure PS. The model deviated significantly from the experimental data at the higher end of the PB concentration range studied here, but it did exhibit the general form of the observed dependence of craze velocity on PB content. © 1993 John Wiley & Sons, Inc.

INTRODUCTION AND MODEL

The toughening of normally brittle glassy polymers has been a topic of interest for many years.[1,2] The high tensile strength, processability, and appearance of glassy polymers such as polystyrene (PS) and polymethylmethacrylate (PMMA) make them very desirable materials, but their low fracture resistance limits their use. Pre-orientation and the inclusion of fibers are effective methods of toughening, but these methodologies have limitations in the production of parts with complex geometries. Toughening may also be achieved through the addition of rubber particles of the appropriate size and compliance[3] that aid in the process of crazing.

For a material that deforms principally via the dilatational mechanism of crazing, toughness, as measured by the area under a stress–strain curve, is approximately the product of the craze flow stress, σ_c, and the strain to fracture, ϵ_f. Therefore, high values of ϵ_f are desired to achieve a tough polymer. The strain rate response of a polymer deforming entirely by crazing may be written[4] as the product of the craze front density, ρ, the craze velocity, v, and b, a parameter related to the amount of dilatation in the material:

$$\dot{\epsilon} = \rho v b \qquad (1)$$

To prevent fracture, the right-hand side of this equation must match the imposed strain rate, $\dot{\epsilon}$. This can be accomplished in two ways. One method is to increase the number of crazes growing in the sample, thereby increasing ρ. The high levels of toughness found in high-impact polystyrene (HIPS), acrylonitrile–butadiene–styrene copolymer (ABS), and blends containing polystyrene–polybutadiene copolymer rely on this technique.[5] The rubber particles, which graft to the glassy phase, are compliant enough to act as craze initiation sites.[6,7] Strain levels on the order of 40–60% are achieved by a large volume density of short crazes. Another method of increasing the strain rate response of the material is to increase the velocity of the growing crazes. This latter phenomenon was examined in this work in an

attempt to explain the unexpected toughness of certain homopolymer blends of polystyrene and polybutadiene (PB). The incorporation of a few weight percent of low molecular weight polybutadiene into high molecular weight polystyrene resulted[8] in decreased craze flow stresses and increased toughness. It has been postulated that the polybutadiene, which phase separates into small homogeneous pools, acts as a plasticizer when placed under stress only in the region of a growing craze, and thus reduces the local plastic resistance of the glassy phase. This local plasticization, in principle, should enable crazes to propagate at higher than expected velocities at relatively low stresses, thereby reducing the statistical probability of premature catastrophic failure of any given craze from extrinsic imperfections.[8] The enhanced toughness arises, therefore, from the material's ability to undergo very high levels of dilatational strain without premature fracture.

Craze growth in brittle glassy polymers can be described by the interface convolution mechanism.[9] In this model the craze growth rate is governed by the strain-rate-dependent tensile plastic resistance, $\hat{Y}$, of the polymer. The incorporation of low molecular weight diluent into the glassy phase lowers the plastic resistance and increases the rate of craze growth under a given stress. As a craze intersects a field of precipitated polybutadiene pools of diameter a, the PB is solubilized under the prevailing negative pressure existing both ahead of the growing craze and on the craze borders.[10] This is shown schematically in Figure 1. Two requirements of this mechanism are that the PB drains onto the surface layer of the growing craze and that it is quickly sorbed into the deforming surface layer during the deformation. The resulting plasticized region is more easily drawn into craze matter. Note that if the PB pools are too large the resulting tapped cavity can act as a critical flaw, which can lead to craze fracture.[8]

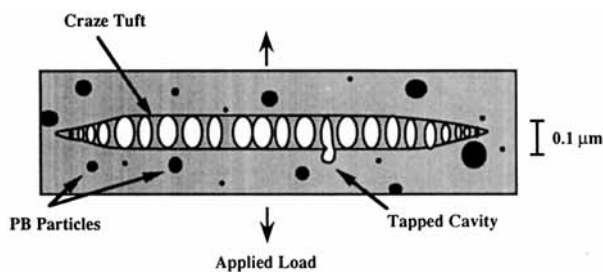Argon and Salama[9] have constructed a model based on the Taylor meniscus instability mecha-

Figure 1 Schematic of growing craze intersecting a field of precipitated polybutadiene pools.

nism, which describes the velocity of crazes in glassy polymers under the influence of the far field stress, σ_∞, as

$$\nu = D_1\exp\left\{-\frac{B}{kT}\left[1 - \left(\frac{\sigma_\infty\lambda'}{\hat{Y}_0}\right)^{5/6}\right]\right\} \quad (2)$$

where $\lambda' = \lambda_n/(1 + Y_h(\lambda_n)/Y_0$, Y_h is the orientation hardening component of the plastic resistance at the craze extension ratio λ_n, Y_0 is the tensile yield strength of the unoriented polymer, and $\hat{Y}_0$ is the athermal plastic resistance of the pure polymer. B is a characteristic activation energy for a unit conformational transition in a plastically relaxing cluster, and D_1 is a parameter defined as

$$D_1 = \frac{9\pi^2 n \chi \dot{\epsilon}_0}{(1 + 2n)2^{1-n}\sigma_\infty\lambda'} \quad (3)$$

where χ is the surface energy of pure PS, $\dot{\epsilon}_0$ is a preexponential frequency factor in the plastic strain rate expression, and n is a plastic strain rate exponent. Based on the Cohen–Turnbull free volume model[11] of viscous resistance it can be expected that the plastic resistance of a glassy polymer should depend on the sorbed fraction, ω, of PB as

$$\hat{Y} = \hat{Y}_0\exp(-\beta_2\omega) \quad (4)$$

where β_2 is a constant not determinable a priori in the present model, and will be considered as adjustable. The sorbed fraction of rubber, ω, must be considered in two parts: ω_c, the soluble weight fraction of rubber; and f, the weight fraction that phase separates. The combination of eqs. (2) and (4) with the appropriate expression for ω furnishes a modified expression for the craze velocity in the presence of prepackaged diluent:[10]

$$\nu = D_1\exp\left\{-\frac{B}{kT}\left[1\right.\right.$$
$$\left.\left. - \left(\frac{\sigma_\infty\lambda'}{\hat{Y}_0\exp[-\beta_2(\omega_c + 16af\,\sigma_\infty/3\pi^2\alpha C)]}\right)^{5/6}\right]\right\} \quad (5)$$

In this expression, α is a parameter indicative of the penetration depth of the PB into the surface layer of the craze matter, and C is a constant arising from the fundamental result of the interface convolution mechanism, which predicts that the product of the imposed stress and the tuft diameter is a constant.

When the craze strain rate equals the imposed strain rate, the far-field stress becomes the craze

flow stress. Rearrangement of eq. (5) then produces an expression for the craze flow stress for heterogeneous blends, $f > 0$:[10]

$$\frac{\sigma_c}{\sigma_{0c}} = \exp\left[-\left(\frac{16\beta_2 a}{3\alpha\pi^2 C}\right)(\sigma_c f)\right] \qquad (6)$$

The corresponding expression for the craze flow stress in the homogeneous regime, $\omega < \omega_c$, is[10]

$$\frac{\sigma_c}{\sigma_0} = \exp(-\beta_2\omega) \qquad (7)$$

In these equations, σ_{0c} is the craze flow stress at the solubility limit and σ_0 is the craze flow stress for pure polystyrene. Craze velocities for blends containing a weight fraction f of precipitated PB can therefore be described with four parameters: β_2 and α, which can be determined from craze flow stress experiments on homogeneous [eq. (7)] and heterogeneous [eq. (6)] blends; and B and λ', which can be determined from craze velocity measurements made on pure polystyrene. In this study we have measured craze velocities in PS–PB blends and compared the results to eq. (5) in an attempt to verify the proposed theory of localized plasticization.

EXPERIMENTAL

The polystyrene used in these blends was Polysar 101, with M_w = 249,000 g/mol and M_n = 111,000 g/mol. The low molecular weight polybutadiene was obtained from Scientific Polymer Products, with M_w = 2300 g/mol and a vinyl content of 29%. The blends were prepared via a precipitation technique that produces a fine powder and which is effective in controlling the polybutadiene particle size distribution.[12] The precipitated and dried powder was compression molded at 200°C for 5 min into a 0.5-mm-thick film, annealed for 24 h at 100°C, then milled into dogbone samples with a gauge length of 6.35 mm and a width of 2.5 mm. The edges and faces of these samples were sanded with 600 grit sandpaper, carefully polished with 5-, 0.3-, and 0.05-μm alumina slurry, washed in a dilute Ivory soap solution to remove residual oils, rinsed with distilled water, and hung vertically in a vacuum oven for 24 h at 80°C. Craze growth specimens were indented with a Leitz microhardness tester to provide controlled craze initiation sites.[13] The microscope attachment on the microhardness tester was used to verify the specimen width at the indentation site.

Care was taken to position the indentations along the principle symmetry axis of the specimen to avoid spurious bending stresses.

Stress–strain results and craze flow stress data were collected at 25°C with an Instron 4201 tensile tester operating at strain rates of 2.6×10^{-4} and 2.6×10^{-3} s^{-1}. Craze growth measurements were made with the apparatus described in previous publications.[13–15] Samples were subjected to a dead load, which provided a constant craze flow stress. A Nikon AT camera, modified to be triggered through the hot shoe, was fired at timed intervals with an Apple computer. The difference in the refractive index between the craze and the undeformed regions allows photography of the surface image of the craze, which appears as a dark stripe. Craze lengths were determined as a function of time to obtain velocities at each imposed stress. A calibration grid was used to scale the craze lengths.

Craze growth measurements were conducted on blends containing 0–5 wt % PB over a stress range of 10–40 MPa. Due to the sensitivity of crazes to residual stress, craze velocity measurements are subject to a great deal of scatter. While steps were taken to minimize the amount of residual stress in these samples, significant scatter was still evident, but not more than in other published studies.

Figure 2 shows four photographs taken from a craze growth experiment performed on a pure PS sample coated with a layer of PB. Crazes grow from a diamond-shaped nucleation site produced by the microhardness tester. The microhardness tester provides a reproducible flaw site, which removes the dependence of the craze propagation rate on the aspect ratio of the flaw. Several researchers have commented on the need to control the aspect ratio, which controls the stress level at the tip of the flaw.[16,17] We can therefore be assured that velocities will be affected only by the applied stress and PB content. The craze length is measured from the diamond to the tip of craze edge. From a series of such measurements, a length versus time plot can be constructed, as shown in Figure 3. Craze length varied linearly with time for the majority of the lifetime of the craze in every experiment. This is consistent with the results found by Argon and Salama.[9] However, nonlinear craze growth has been reported by several investigators. Both Regel[18] and Sato[19] found a linear dependence between length and log time. Sato also observed that crazes stopped growing after a period of time, a result that was attributed to the onset of yielding, which would effectively blunt craze growth. Sauer and Hsaio[20] recorded linear growth with time, but only beyond a critical length. The

latter results are similar to observations made in our experiments. An initial "startup" period is often seen in which craze growth is nonlinear, which we attribute to residual stress surrounding the craze initiation site. In our samples, this residual stress is evidenced by a small amount of birefringence around the nucleation site. Once the craze has propagated beyond this birefringent zone, linear craze growth commences. A decrease in velocity after a certain period of time has also been observed in some of our experiments, although not to the point of complete cessation as reported by Sato. Velocities generally decreased whenever there was encroachment by other crazes. The presence of another craze could lower the far-field stress experienced by the isolated craze, thereby slowing its propagation. Spurr and Niegisch[21] observed arrested craze growth at long times only in samples crazed at higher stresses. They

further noted a larger craze density at higher stresses, which would suggest that the presence of another craze in close proximity is enough to reduce the stress field in a growing craze. Kambour[22] has stated that when two crazes are close enough to impede each other's growth, curved growth trajectories would result followed by mutual craze termination. This particular phenomenon was, however, not observed in our experiments. Theoretical work by Knight[23] has suggested that linear craze growth occurs when the ratio of the craze length to thickness becomes sufficiently large. He reports a ratio of 300 for PMMA. In our samples, we estimate a length-to-width ratio of this same order. From the slope in the linear region in plots like Figure 3, a craze velocity can be obtained as a function of the far-field stress. Craze velocity measurements were also made on samples of PS with a liquid layer of
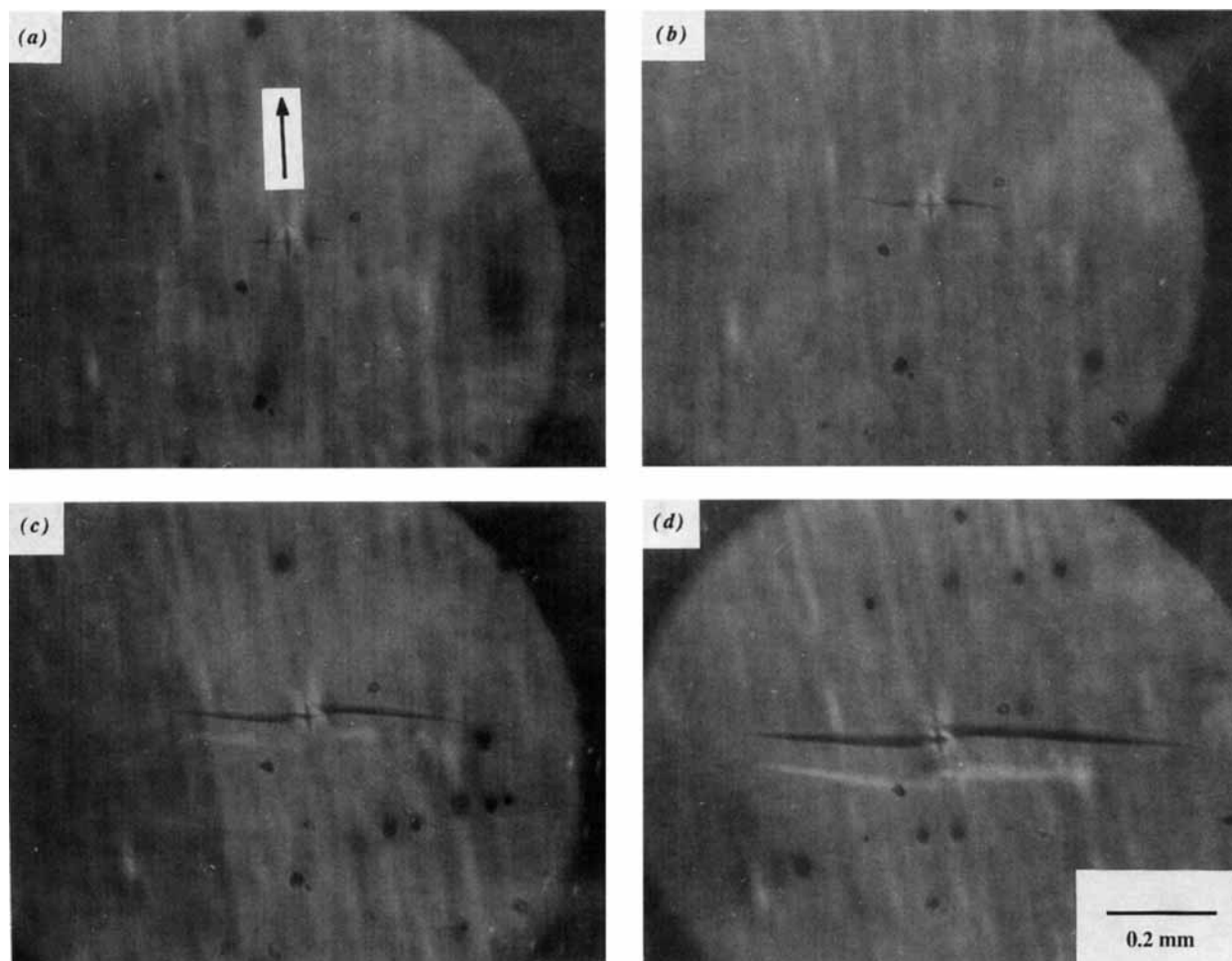

Figure 2 Craze growth length as a function of time for polystyrene coated with polybutadiene at an applied stress of 10.7 MPa. (a) 30 s, (b) 1.5 min, (c) 3.5 min, (d) 6.0 min. Arrow indicates direction of applied stress.
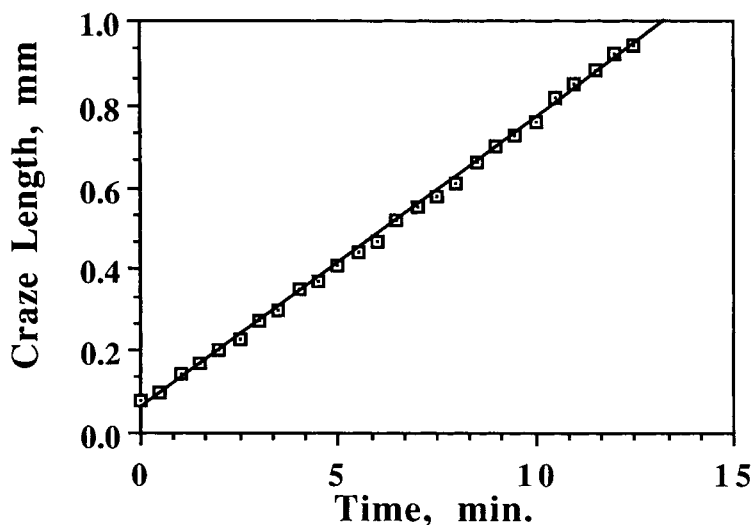
Figure 3   Craze length as a function of time for PS-coated with polybutadiene under an applied stress of 10.7 MPa. Craze velocity: 1.2×10^{-6} m/s.

PB on the surface, with the intention of supplying a growing craze with an infinite supply of PB. To obtain this, a drop of PB was placed on a microscope cover slip that was then pressed against the indented PS surface. The cover slip held the PB in place while providing an optically smooth surface.

RESULTS AND DISCUSSION

The effect of PB incorporation in PS on the observed level of toughness is demonstrated in the stress–strain results for the polybutadiene–polystyrene blends presented in Figure 4. As the PB content increases, the craze flow stress decreases while the strain-to-fracture increases. Toughness, or the area under the stress–strain curve, monotonically increases with PB content up to 4% PB. The fact that the modulus remains fairly constant for all the blends confirms the hypothesis that the PB locally plasticizes the PS rather than resulting in significant bulk plasticization. The strain-to-fracture reaches a maximum of 40% in the blend containing 4% PB at a flow stress of 24 MPa. A typical high-impact
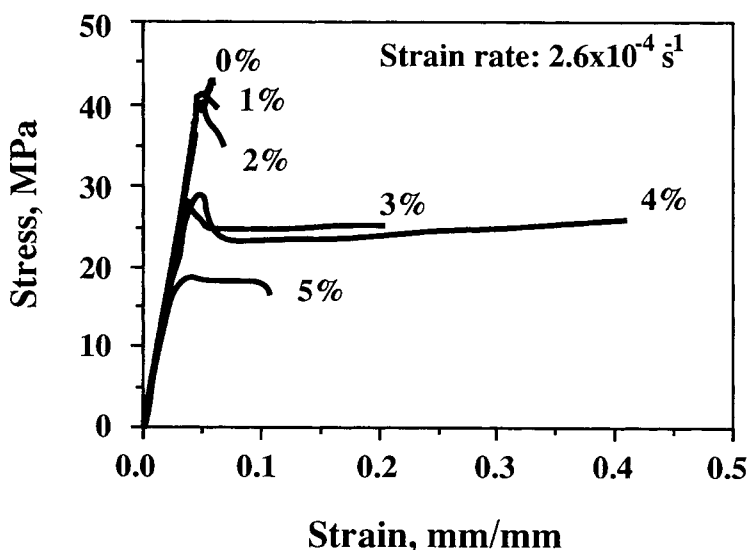

Figure 4   Stress–strain behavior of PS–PB blends as a function of weight percent of PB. Strain rate: 2.6×10^{-4} s^{-1}.

polystyrene (HIPS) at approximately the same strain rate has a strain-to-fracture of 25% and a flow stress of 22 MPa.[24] Above 4% PB content, the size distribution of the PB pools broadens significantly and larger, micron-sized PB pools act as critical flaws, which lead to premature fracture when such pools are drained by an advancing craze.[8]

It was necessary to estimate the four unknown constants in eq. (5) before the model could be compared with experimental craze velocities in the PB–PS blends. Two of the parameters, β_2 and α, were determined from craze flow stress measurements on

the blends. Craze flow stress data collected at ambient conditions are plotted as a function of PB content in Figures 5(a) and 5(b). Results from two strain rates are represented. Equations (6) and (7) are plotted against the data for the slower strain rate in Figure 5(a). The solubility limit, ω_c, was 0.4% as determined from transmission electron microscopy performed on osmium-tetroxide-stained samples. Note that ω_c is expected to be a function of the polybutadiene microstructure and the molecular weight of both components. From a comparison of eq. (7) with the data below the solubility limit, a
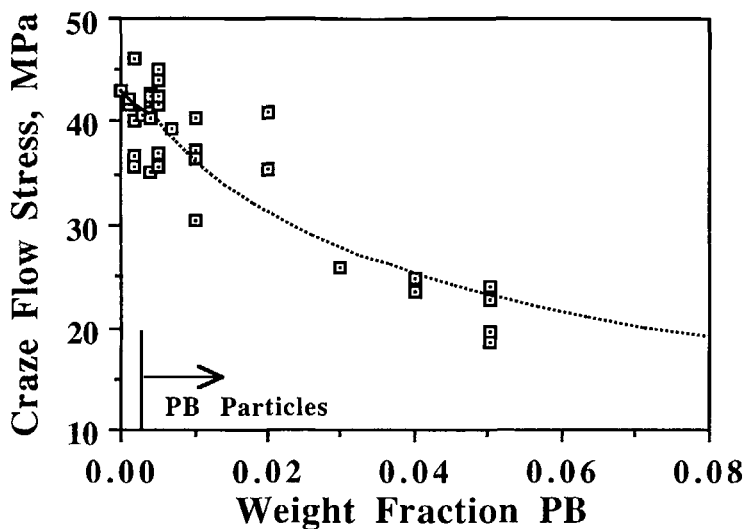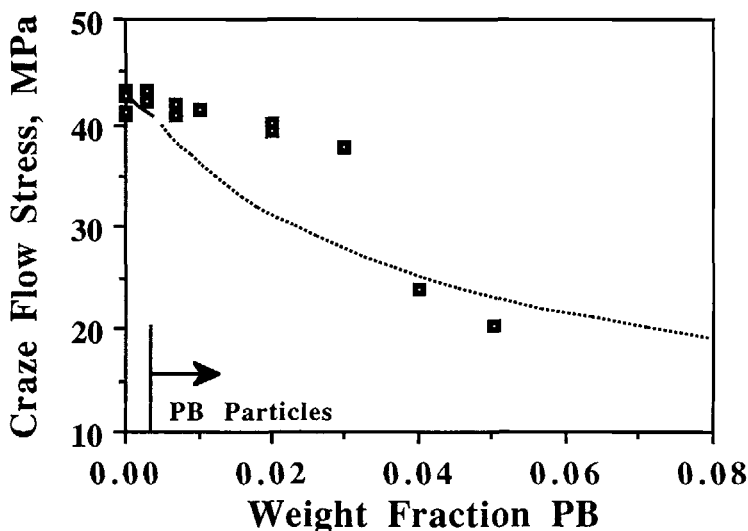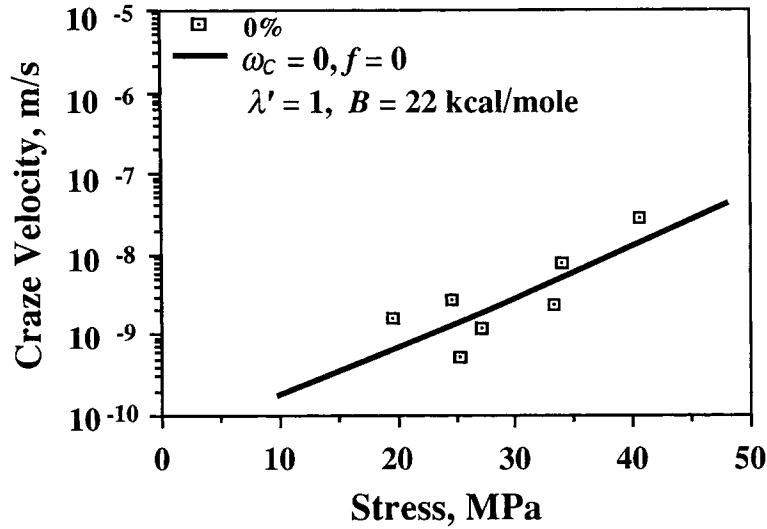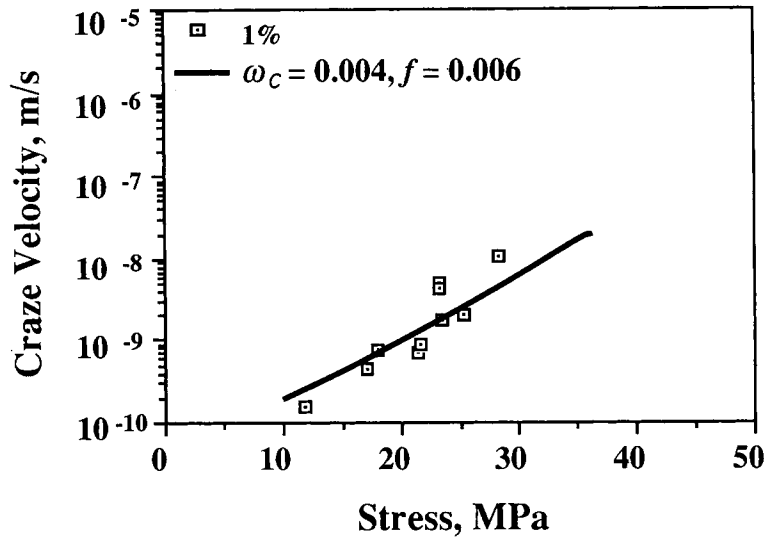

Figure 5   Craze flow stress as a function of polybutadiene content. Dashed line represents behavior predicted by Eqs. (6) and (7). (a) Strain rate 2.6×10^{-4} s^{-1}, (b) strain rate 2.6×10^{-3} s^{-1}.

Figure 6 Craze velocity data for PB–PS blends compared with modified interface convolution model: (a) pure PS, $\omega_c = 0$, $f = 0$; (b) 1% PB, $\omega_c = 0.004$, $f = 0.006$; (c) 3% PB, $\omega_c = 0.004$, $f = 0.026$; (d) 5% PB, $\omega_c = 0.004$, $f = 0.046$.

value of 13 was determined for β_2. This value for β_2, an average pool diameter a of 0.09 μm as determined from TEM, and a value[10] of 2.5×10^{-7} MPa-m for C were substituted in eq. (6), which was then compared with the craze flow stress data above the solubility limit to give a value of 5 for α. As was previously found,[10] this value is much larger than anticipated and suggests deep penetration of the PB into the craze material.

Craze flow stress is dependent on strain rate, as has been previously shown.[12] As shown in Figure

5(b), a faster strain rate results in a shift to the right, which changes the determined values of β_2 and α. This shift is believed to result from limitations on the rate of diffusion of the PB into the fringing layer of the growing craze, which would reduce the amount of localized plasticization observed. The flow stress will consequently decrease more slowly with PB content than the series of samples tested at the slower strain rate. For the purpose of this analysis, however, the values for β_2 and α found from the slower strain rate data will be used in the
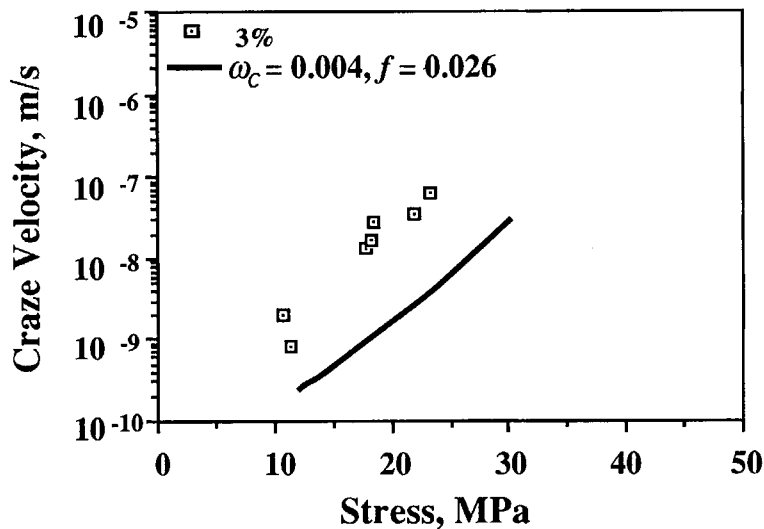
(c)
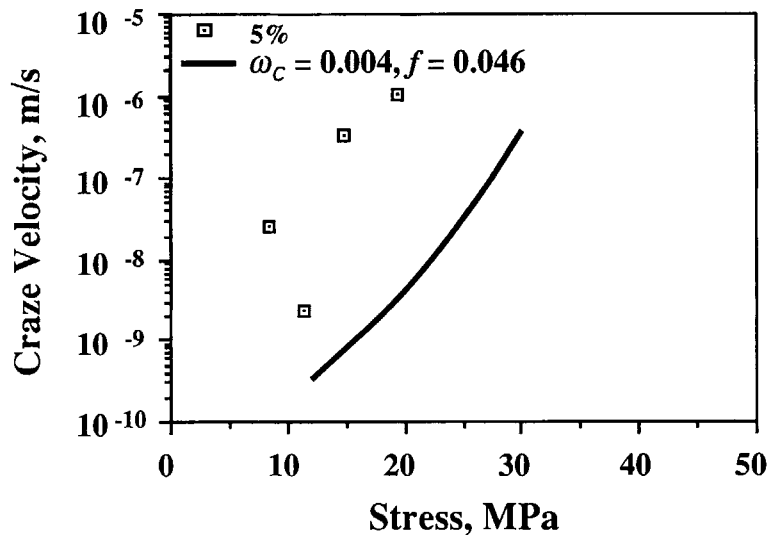
(d)

Figure 6 *(Continued from the previous page)*

velocity expression. Clearly these values only serve as estimates, but it is nevertheless apparent that the general form of the craze flow stress dependence on PB content is captured by eqs. (6) and (7).

The two remaining parameters in the model, B and λ', were determined from the data for pure polystyrene [Fig. 6(a)]. Values of 22 kcal/K and 1.0 were found for B and λ', respectively. These are somewhat different from the values obtained by Argon and Salama,[7] who found values of 25 kcal/K and 1.9. Their PS, however, was slightly more polydisperse, which could explain the difference in these

parameters. These values, along with the previously determined parameters, β_2 and α, were then used to construct the velocity trends predicted by the model [eq. (5)].

A series of craze velocity versus stress data was obtained for PS samples containing 0, 1, 3, and 5 wt % PB. The results from all these tests are plotted on a semilog plot in Figure 6 along with the trend predicted by the model [eq. (5)]; the values of the model parameters are tabulated in Table I. For PB contents in the region of 1%, the model follows the data with a fair degree of accuracy. At higher PB

Table I   Parameters for Craze Velocity Model

Y_0	248 MPa	$\dot{\epsilon}_0$	10^{13} s^{-1}
a	0.09 μm	β_2	13
C	2.5×10^{-7} MPa-m	α	5
χ	5×10^{-2} J/m^2	B	22 kcal K
n	0.05	λ'	1

data. This suggests that the model does not take into account all the phenomena occurring in the locally plasticized crazing process and therefore requires some modification to better account for the effects of concurrent deformation and sorption, and for the rate of spreading of the liquid PB on the craze surfaces.

concentrations, however, the model, while showing the general increasing trend of velocity with PB content, predicts a smaller slope and hence a weaker dependence of velocity on PB than observed in the

Transmission electron microscopy studies performed on these blends show that the PB pool size obtained from our blending technique is independent of PB content up to 5% where a bimodal distribution appears as previously mentioned. The average dis-
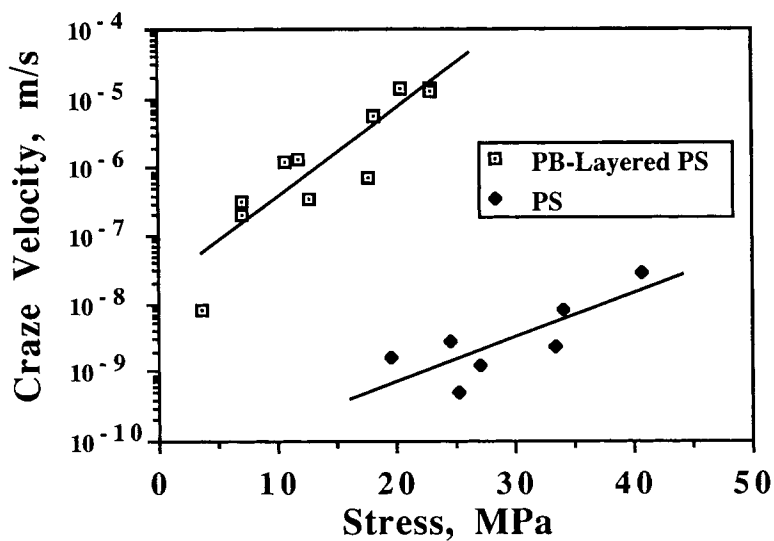
(a)
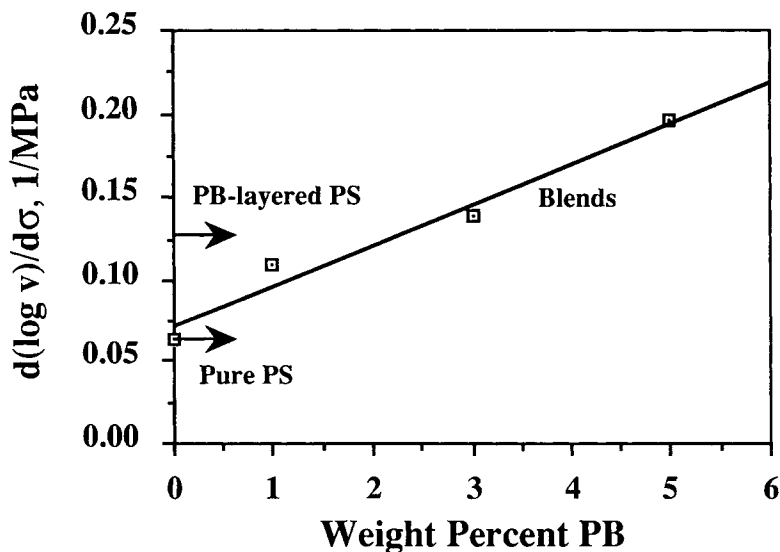
(b)

Figure 7   (a) Craze velocity data for PB-coated polystyrene and pure polystyrene. (b) Best-fit slope of craze velocity–stress data for PB–PS blends and PB-layered PS.

tance between PB pools therefore decreases with PB content, which suggests that a craze can sample more pools in a given area at higher PB contents. This spatial dependence also needs to be accounted for in the model.

The effect of PB content on craze velocity in these blends can be seen when viewing the results in Figures 6(a)-(d) at one stress level. At a stress of 18 MPa, pure PS and the 1% blend have craze velocities on the order of 8×10^{-10} m/s. At this same stress level, the 3% blend has a velocity of 1×10^{-8} m/s, while the 5% blend rises to 7×10^{-7} m/s. Therefore, we have demonstrated an increase in craze velocity of roughly 3 orders of magnitude accompanied by a negligible change in macroscopic modulus from pure PS, which supports the concept of localized plasticization of crazes. This enhanced velocity increases the sample's ability to match imposed strain rates at lower flow stresses, and thereby achieve a higher strain-to-fracture and hence a higher level of toughness. The fact that the 5% blend, which showed a decreased toughness from the 4% blend, exhibits a higher velocity confirms the hypothesis that this toughness decrease is due to the appearance of larger PB pools that act as supercritical flaws.

Sauer and Hsaio[20] observed velocities for pure PS between 5×10^{-10} and 1×10^{-9} m/s over a stress range of 17–22 MPa, which are consistent with our observed data. These values were obtained from measurement of craze penetration depths as viewed from the opposite side of the specimen. The fact that the velocities are close to our observed velocities suggests that the velocity of the craze front along the surface of the specimen, which was measured in

our experiments, is a good representation of the behavior of the entire craze.

Craze velocity measurements were also performed on PS samples with a layer of PB on the surface, the results of which are shown in Figure 7(a). These experiments were intended to provide an upper bound to the PB–PS blend velocities, as each craze should have an unlimited supply of PB. While the measured craze velocities were indeed higher in these samples than in any of the blends studied (1 order of magnitude faster than the 5% blend), the stress dependence of the craze velocity is significantly lower than the 3 and 5% blends; a plot of the semilog velocity–stress slope as a function of PB content is shown in Figure 7(b) along with the limiting values for pure PS and PB-layered PS. One possibility for the lower-than-expected slope for the PB-coated sample is a transport limitation of the PB from the external surface to the craze surface at high stress levels, which correspond to high strain rates. Thus, the craze front in the interior of the PB-layered PS specimen may be starved of PB, while the craze front along the surface would continue to be supplied with fresh PB. The reduced craze propagation rate in the interior of the sample would therefore be expected to result in long, shallow crazes with a depth-to-width ratio less than 0.5, as suggested in Figure 8(a). The constrained craze front in the interior would slow the propagation of the surface craze front, which would decrease the overall observed craze velocity at higher stresses.

This hypothesis was evaluated with the setup shown in Figure 8(b). Crazed samples were held under tension at an angle between 25 and 65° in an
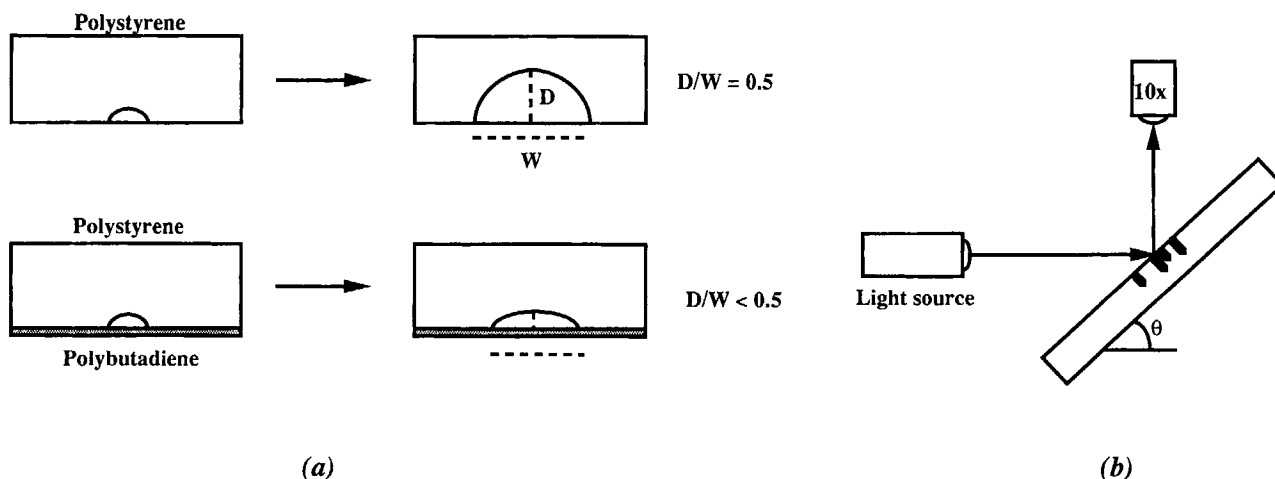

(a)   *(b)*

Figure 8   (a) Craze propagation behavior in pure PS samples and PB-layered PS samples as viewed parallel to the stress axis. (b) Schematic of depth of penetration study.

optical microscope so that the crazed surface was visible. Reflected light illuminated the crazes in the sample. Figures 9(a) and 9(b) show the results for pure PS and PB-layered PS. Measurements of craze depth were corrected with Snell's law to account for refraction effects. Corrected craze depth versus width results are shown in Figure 10. Crazes grown in pure PS show an aspect ratio equal to or greater than 0.5. Aspect ratios larger than 0.5 may be caused from the difference in the coefficient of thermal expansion between PS and the molding plates, which would result in residual compressive stresses on the sample surface. Additional errors could result from

difficulties in determining the exact craze shape in the optical measurements. The PB-layered PS samples, however, consistently showed aspect ratios less than 0.5, which supports the hypothesis of transport limitations and represents a rationale for the lower-than-expected slope in Figure 7(a) for the PB-layered samples.

These results also reinforce the importance of having well-dispersed PB pools throughout the specimen. Thus, there should always be sufficient PB in the immediate vicinity of a growing craze to reduce transport limitations. As suggested previously, a decrease in the spatial distance between PB
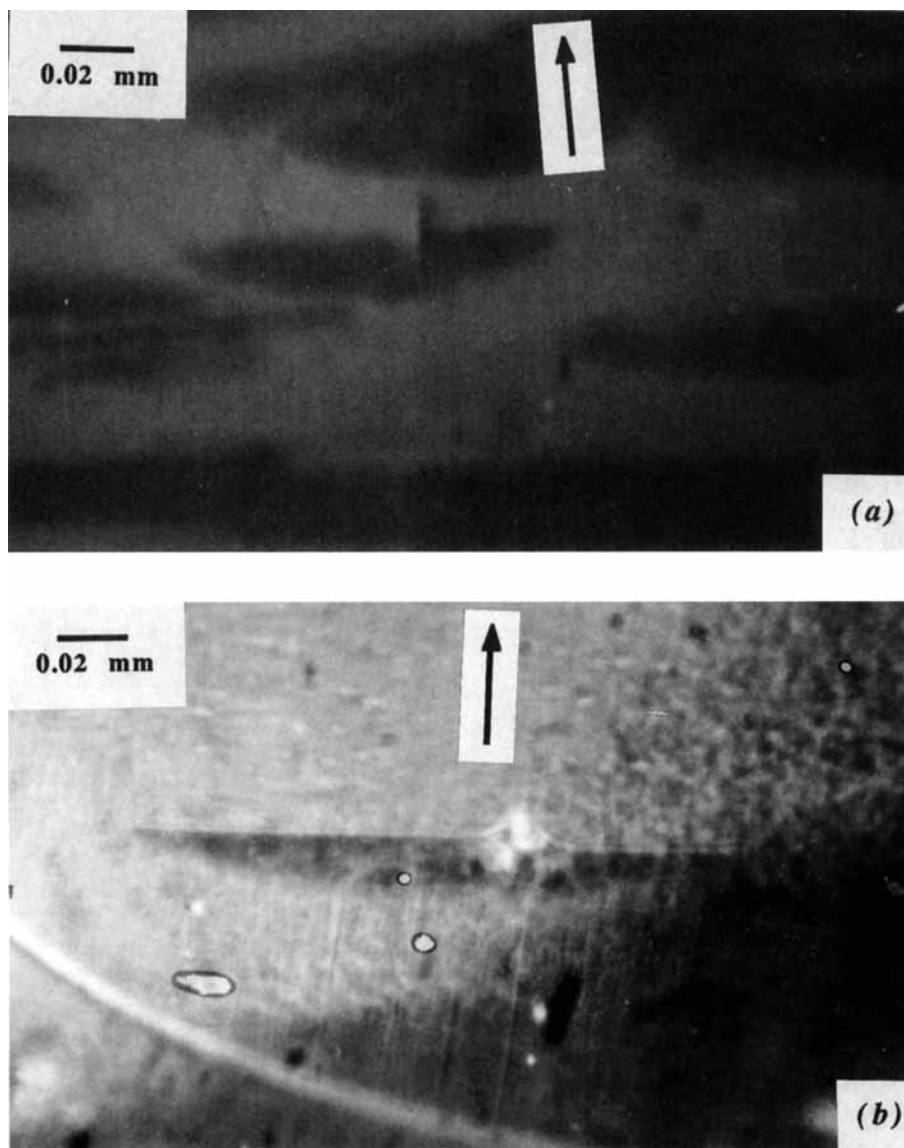

Figure 9 Crazes viewed at angle under reflected light: (a) pure PS, (b) PB-layered PS. Arrow indicates direction of applied stress.
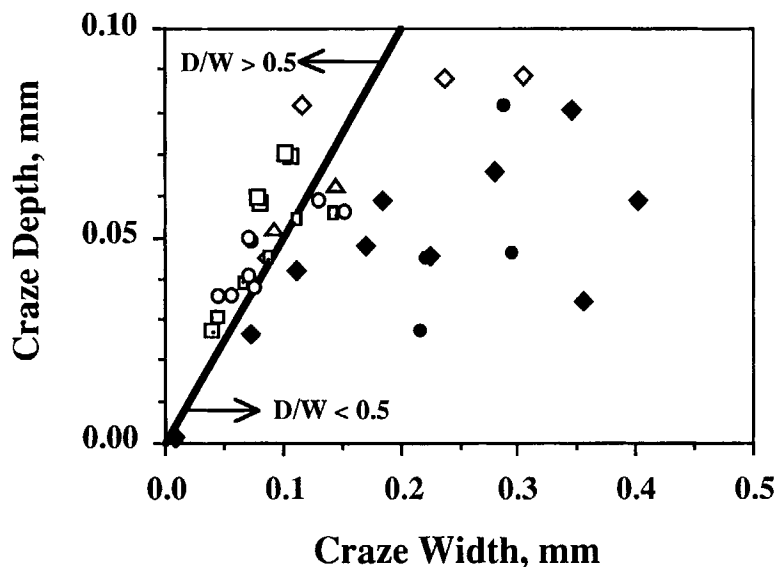
Figure 10 Craze depth as a function of craze width for pure PS and PB-layered PS. Results for PB-layered PS are shown with black data points; results for PS are shown with white data points.

pools should result in high craze velocities and hence tougher blends. The craze velocity results suggest that it is the appearance of larger pools of PB that lead to premature fracture in the 5% blend, not velocity limitations. We can conclude, therefore, that the limits of toughening provided by this new mechanism of localized craze plasticization have not yet been realized, and that better control of PB pool size could result in even tougher materials that perform well at strain rates above 10^{-1} s^{-1}.

CONCLUSIONS

We have shown that the incorporation of a few weight percent of low molecular weight PB with adequate fluidity into polystyrene results in greatly enhanced craze velocities which, in turn, enhance toughness in certain regimes of strain rate. The phenomenon of local plasticization of growing crazes lowers the craze flow stress and increases the craze velocity without significantly affecting the modulus. Better control of PB pool size may result in yet higher levels of toughness. This may be achieved with still lower molecular weight diluents whose structures allow them to phase separate from the glassy polymer at small weight percents; the reduced molecular weight diluent may also help to circumvent the strain rate limitations on this toughening mechanism through an increased diffusion rate of the diluent through the glassy phase.

We have also tested a model that accounts for the plasticizing effects of the diluent on the craze velocity. While the model followed the general trend of the data, it is apparent that some modification is needed to capture the observed stress and diluent concentration dependence of the craze velocities in these blends.

REFERENCES

1. A. S. Argon and R. E. Cohen, *Advances in Polymer Science*, 91/92, Springer-Verlag, Berlin, Heidelberg, 1990, pp. 302–351.
2. C. B. Bucknall, *Toughened Plastics*, Applied Science Publishers, London, 1977.
3. E. Piorkowska, A. S. Argon, and R. E. Cohen, *Macromolecules*, **23**, 3838 (1990).
4. A. S. Argon, R. E. Cohen, O. S. Gebizlioglu, and C. E. Schwier, *Advances in Fracture Research*, Pergamon Press, Vol. 4, New York, 1984, p. 427.
5. C. B. Bucknall and R. R. Smith, *Polymer*, **6**, 437 (1965).
6. E. Piorkowska, A. S. Argon, and R. E. Cohen, to appear.
7. M. E. Boyce, A. S. Argon, and D. M. Parks, *Polymer*, **28**, 1680 (1987).
8. O. S. Gebizlioglu, H. W. Beckham, A. S. Argon, R. E.

Cohen, and H. R. Brown, *Macromolecules,* **23,** 3968 (1990).

9. A. S. Argon and M. M. Salama, *Phil. Mag.,* **36,** 1217 (1977).
10. A. S. Argon, R. E. Cohen, O. S. Gebizlioglu, H. R. Brown, and E. J. Kramer, *Macromolecules,* **23,** 3975 (1990).
11. M. H. Cohen and D. Turnbull, *J. Chem. Phys.,* **31,** 1164 (1959).
12. J. Qin, A. S. Argon, and R. E. Cohen, to appear.
13. G. W. Hawkins, Ph.D. Thesis, Massachusetts Institute of Technology (1983).
14. J. A. DiCorleto and R. E. Cohen, *Polymer,* **29,** 1245 (1988).
15. C. E. Schwier, A. S. Argon, and R. E. Cohen, *Phil. Mag.,* **52,** 581 (1985).
16. S. S. Sternstein and K. J. Sims, *ACS Polymer Preprints,* **5,** 422 (1964).
17. G. P. Marshall, L. G. Culver, and J. G. Williams, *Proc. Roy. Soc. Lond., A.,* **319,** 165 (1970).
18. V. R. Regel, *Tech. Phys., USSR,* **1,** 895 (1953).
19. Y. Sato, *Kobunshi Kagaku,* **23,** 69 (1966).
20. J. A. Sauer and C. C. Hsaio, *ASME Trans.,* **75,** 895 (1953).
21. O. K. Spurr and W. D. Niegisch, *J. Appl. Polym. Sci.,* **6,** 585 (1962).
22. R. Kambour, *J. Polym. Sci., Part D Rev.,* **7,** 1 (1974).
23. A. C. Knight, *J. Polym. Sci., Part A,* 1845 (1965).
24. A. S. Argon, R. E. Cohen, and O. S. Gebizlioglu, in, *Mechanical Behavior of Materials–V,* M. G. Yan et al., Eds., Pergamon Press, New York, Vol. 1, 1987, p. 3.